



**HAL**  
open science

# Time-dependent atomic diffusion in magnetic ApBp stars

M. Stift, G. Alecian

► **To cite this version:**

M. Stift, G. Alecian. Time-dependent atomic diffusion in magnetic ApBp stars. Monthly Notices of the Royal Astronomical Society, 2016, 457 (1), pp.74-81. 10.1093/mnras/stv2962 . hal-02339142

**HAL Id: hal-02339142**

**<https://hal.science/hal-02339142v1>**

Submitted on 8 Dec 2023

**HAL** is a multi-disciplinary open access archive for the deposit and dissemination of scientific research documents, whether they are published or not. The documents may come from teaching and research institutions in France or abroad, or from public or private research centers.

L'archive ouverte pluridisciplinaire **HAL**, est destinée au dépôt et à la diffusion de documents scientifiques de niveau recherche, publiés ou non, émanant des établissements d'enseignement et de recherche français ou étrangers, des laboratoires publics ou privés.

# Time-dependent atomic diffusion in magnetic ApBp stars

M. J. Stift<sup>1,2,3★</sup> and G. Alecian<sup>2</sup>

<sup>1</sup>Armagh Observatory, College Hill, Armagh BT61 9DG, UK

<sup>2</sup>LUTH, Observatoire de Paris, CNRS, Université Paris Diderot, 5 Place Jules Janssen, F-92190 Meudon, France

<sup>3</sup>Universität Wien, Universitätsring 1, A-1010 Wien, Austria

Accepted 2015 December 17. Received 2015 December 16; in original form 2015 October 23

## ABSTRACT

Numerical modelling of surface abundance distributions in ApBp star atmospheres constitutes a challenging astrophysical problem. This paper is intended to deepen our understanding of how atomic diffusion affects the atmospheric structure of magnetic ApBp stars, and in particular how time-dependent calculations may be compared to the alternative method of estimating equilibrium stratifications. Our numerical calculations – with the stellar atmosphere adjusted self-consistently to the abundance profiles – show that final stationary solutions of the time-dependent diffusion problem (constant particle flux throughout the stellar atmosphere) are seemingly at variance with equilibrium stratifications (zero particle flux). In this work, we will provide some understanding of the origin of these differences and try to elucidate the as yet little explored behaviour of time-dependent atomic diffusion. To this purpose, we assess the influence of the boundary condition at the bottom of the atmosphere, we investigate how the stratifications depend on magnetic field angle and strength, and we have a look at possible interactions between different chemical elements. Based on a grid of atmospheric models and stratifications reflecting dipolar magnetic geometries, we also present predicted line profiles for different oblique rotator models. Finally, we shortly discuss the consequences of our findings for the interpretation of abundance maps of magnetic ApBp stars.

**Key words:** diffusion – line: profiles – stars: abundances – stars: chemically peculiar – stars: magnetic field.

## 1 INTRODUCTION

Recently, Alecian (2015) has presented an in-depth discussion of state-of-the-art *equilibrium* abundance stratifications due to atomic diffusion in magnetic ApBp stars, including an outline of major developments in this field since the seminal paper by Michaud (1970). These equilibrium stratifications (also computed by LeBlanc et al. 2009 in the non-magnetic case) represent the abundance stratifications required to achieve zero diffusion velocities for a given group of elements in the stellar atmosphere. In other words, the module of the radiative acceleration vector must be approximately equal to the module of the gravity vector (usually they are of opposite sign). As shown initially by Vaclair, Hardorp & Peterson (1979), radiative accelerations depend on magnetic field strength and in particular on inclination, revealing that horizontal magnetic field lines must play an important role in the accumulation of chemical elements. Whereas early modelling did not take into account the effects of the stratification of elements like Cr and Fe on the atmospheric structure, Stift & Alecian (2012) established self-consistency between model atmosphere and vertical abundance distributions by combin-

ing Kurucz’s ATLAS12 code (Kurucz 2005; Bischof 2005) with their CARAT code (Alecian & Stift 2006) in an iterative procedure. They also had a short look at the mutual interactions between the various chemical elements. Please note that the numerical modelling presented in this paper has been carried out under the assumption of local thermodynamic equilibrium and that the effect on ions of the ambipolar diffusion of hydrogen (Babel & Michaud 1991) is neglected. Only vertical diffusion velocities are considered for the reasons discussed in section 4.1 of Alecian & Stift (2006).

At about the same time, Alecian, Stift & Dorfi (2011) presented first results on the time-dependent build-up of element stratifications in magnetic ApBp star atmospheres. Stift, Alecian & Dorfi (2013a), using their CARATSTRATMOTION code, extended these calculations to more realistic, self-consistent models of time-dependent atomic diffusion of iron-peak elements at various field strengths and field angles. As it turned out, important differences are found between equilibrium stratifications and the final stationary stratifications resulting from the evolution in time of diffusion, abundances and atmospheric structure, as shown in fig. 5 of Alecian et al. (2011). It also became clear that huge abundance gradients can develop in the presence of (almost) horizontal field lines – even when these are of modest strength – and that these would engender temperature inversions in higher atmospheric layers. Keeping in mind that the

\* E-mail: martin.stift@univie.ac.at

two approaches (time-dependent and equilibrium) do not involve the same set of equations, one will not be surprised to find that they lead to different abundance stratifications, a point which will be discussed in Section 3.

Given the large differences between final stationary stratifications in the time-dependent case on the one hand and the equilibrium stratifications underlying the interpretation of virtually all non-standard abundances found in ApBp stars on the other hand, we deemed it important to study time-dependent diffusion in more detail. Among others, we had to deal with the question of how far towards  $90^\circ$  in field angle can we go in our simulations before (numerical) instabilities set in. In addition, we had to elucidate how the boundary conditions influence the final stationary solutions (Section 4) and whether the interactions between the various chemical elements are important (Section 6). The dependence on field strength of the stratification profiles also had to be explored (Sections 5 and 7). In order to provide observational predictions, we finally decided to attempt the modelling of spectral lines and their variability, based on the theoretical stratifications and fairly simple magnetic geometries (Section 7.1).

## 2 TIME-DEPENDENT BUILD-UP OF ABUNDANCE STRATIFICATIONS

Time-dependent diffusion calculations in stellar atmospheres present specific difficulties not encountered in stellar interiors which have the advantage of being optically thick (see for instance Turcotte, Richer & Michaud 1998; Seaton 1999). The numerics of time-dependent atomic diffusion in the atmosphere of a magnetic ApBp star have been discussed in detail by Alecian et al. (2011). The stratification build-up was modelled for the fictitious element ‘cloudium’, specifically designed to allow for fast computation and with atomic properties inspired by those of Hg. Given the few spectral lines and the low abundance of ‘cloudium’, it was not necessary to update the atmosphere. Since time-dependent diffusion of elements like Cr and Fe makes no sense unless it is carried out self-consistently, we significantly optimized our numerical code `CARATSTRATMOTION` and obtained access to more powerful servers, so that we are now able to keep our atmospheric models self-consistent with the stratified abundances, exactly as was done in Alecian (2015) for the equilibrium stratifications. The modelling of time-dependent diffusion of iron-peak elements proves very challenging because many more iterations are required than for the equilibrium solutions: typically we are faced by an increase in computing time by a factor of 10. On the other hand, there are the numerical (and perhaps also physical) instabilities mentioned in the previous section, partly due to the enormous vertical abundance gradients that can develop in horizontal fields, entailing temperature inversions (Stift et al. 2013a) which can no longer be coped with by `ATLAS12`. A sweeping comparison between the results presented in Alecian (2015) and time-dependent calculations thus becomes impossible, and we have to restrict ourselves to a handful of instructive examples.

### 2.1 A stationary solution for $60^\circ$ magnetic line inclination

Fig. 1 shows the time-dependent diffusion of Fe in a  $T_{\text{eff}} = 10\,000$  K model with a magnetic field of 10 kG, inclined by  $60^\circ$  with respect to the surface normal. The evolution of the Fe abundance is shown up to the time (some  $10^5$  years) when a stationary constant particle flux throughout the atmosphere is attained. At time zero the abundance of iron is supposed to be solar and homogeneous. The equilibrium stratification of Fe for the same starting atmosphere is also shown

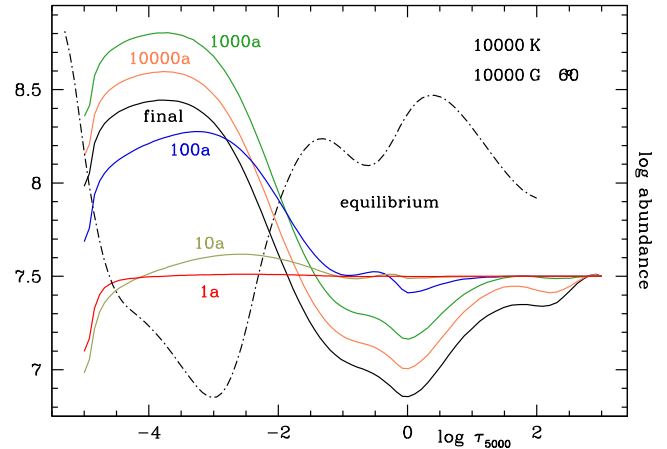


**Figure 1.** Time-dependent diffusion of Fe compared to the equilibrium stratification for a model with  $T_{\text{eff}} = 10\,000$  K,  $\log g = 4.0$  and a magnetic field of 10 kG strength, inclined by  $60^\circ$  with respect to the surface normal. The various curves are labelled with the time in years elapsed since the assumed onset of diffusion. The dash-dotted line gives the equilibrium stratification – the radiative acceleration of Fe is equal to 4.0 throughout the atmosphere.

in the plot. Note that, in order to ensure a self-consistent evolution of stratifications, the `ATLAS12` model has been recomputed once abundances have changed by at most 5 per cent anywhere in the atmosphere in the time-dependent approach. In the convergence towards equilibrium stratifications, the update of the atmosphere is done at each iteration step. In both cases, time-dependent and equilibrium, Fe only was assumed to diffuse for simplicity’s sake.

The high overabundance of iron in layers near  $\log \tau_{5000} \approx -4.0$  (for convenience we shall simply use  $\tau$  in the following) obtained from time-dependent simulations is due to the low diffusion velocity in an inclined magnetic field. The decrease in diffusion velocity becomes much more drastic when the field angle is very close to  $90^\circ$ , but as explained before, the very highest inclinations cannot at present be dealt with. For the discussion in the next section, we have therefore limited ourselves to the  $60^\circ$  case for which we have been able to easily obtain stationary solutions. The stratification reached after some  $10^5$  years of time-dependent diffusion in the atmosphere is completely different from the one required for equilibrium (i.e. zero particle flux). However, we think that this result can well be explained.

## 3 UNDERSTANDING THE DIFFERENCE TIME-DEPENDENT VERSUS EQUILIBRIUM

The stationary solutions we obtain depend mainly on two physical quantities.

(i) The particle flux at the deepest layers, which is one of our boundary conditions. These boundary conditions are posited such that the abundance remains constant with time in the deepest layer; at the top the abundance can evolve freely and particles are allowed to escape from the star. By definition, the stationary solution (the curve labelled *final* in the figure) gives a flux that is constant everywhere. Therefore, an abundance stratification evolves with time until the outgoing particle flux (through the top layer) becomes equal to the incoming flux at the deepest layer. Because the inclination of the magnetic field lines which we have adopted here ( $60^\circ$ ) is still far from horizontal ( $90^\circ$ ), the *door* is still wide open at the upper boundary and the system can adjust the outgoing flux to the

incoming one (lower boundary). For  $90^\circ$ , the *door* will be almost closed at the upper boundary<sup>1</sup> and elements (iron in the present case) become trapped, but not completely so because the neutral state of an atom is insensitive to the magnetic field and can still escape the atmosphere.

However, imagine this trap to be efficient enough – depending on the Fe I fraction – to prevent a significant amount of the element to escape. This implies that the element will accumulate sufficiently in the upper layers to result in almost zero diffusion flux. Such a final stationary solution will be nothing else than a quasi-equilibrium solution imposed on the entire atmosphere. With our code, this solution cannot be perfectly achieved; it would imply that the abundance in the bottom layer has to be changed, something that is not allowed by the algorithm presently implemented. We suggest that one could possibly obtain stratifications close to equilibrium in stellar regions where the magnetic field lines are close to horizontal, and more general stationary solutions elsewhere in the star. Note that non-LTE (absence of local thermodynamic equilibrium) effects can cause a drastic drop in radiative accelerations in high-lying atmospheric layers (Proffitt et al. 1999). This may be another way of forcing a zero outgoing diffusion flux and thus impose equilibrium for the elements concerned in the whole atmosphere, regardless of the magnetic geometry.

(ii) The diffusion time-scale is the second important quantity necessary to understand the stationary time-dependent solutions. Because diffusion time-scales<sup>2</sup> vary roughly as the mass density throughout the atmosphere in the non-magnetic case (see examples of Fe diffusion time-scales in fig. 1 of Alecian 2013a), they are smaller by several orders of magnitude in the upper atmospheric (optically thin) layers than in the deep atmosphere. This is no more the case in a horizontal magnetic field. Diffusion time-scales also depend on radiative accelerations and can – in the case of Fe with solar abundance and in the absence of magnetic fields – be estimated at about 1 year in layers with  $\log \tau \approx -4.0$  and larger than  $10^4$  years in layers with  $\log \tau \approx 2.0$ . As a consequence of this large difference in time-scales, the build-up of abundance stratifications starts first in the upper layers (at least when the inclination of the field lines is not too close to  $90^\circ$ ) and adjusts permanently to the incoming flux from the layers below. Stationarity is fully reached when the deepest layers have adjusted to the incoming flux of the lower boundary.

At a first glance Fig. 1 could appear disturbing, since the equilibrium stratification exhibits a hole in the Fe abundance near  $\log \tau \approx -3.0$ , whereas the time-dependent solution indicates an accumulation. A disagreement in the opposite sense appears around  $\log \tau \approx 0.0$ . It is a fact that the stratification profile of the time-dependent stationary solution (the curve labelled *final* in the figure) is the one ensuring a constant particle flux throughout the atmosphere. However, how can one explain a stationary overabundance in layers where according to the equilibrium stratification iron cannot be supported by the radiation field at such an abundance level? The answer comes from the underabundance formed below  $\log \tau \approx -2.0$  in the time-dependent solution, and its repercussions on iron opacity and radiative acceleration. Since the medium is optically thin above  $\log \tau \approx 0.0$ , in the equilibrium stratification we

find a radiation screening effect due to the Fe overabundance. In contrast, more available photons coming from below  $\log \tau \approx -2.0$  support the overabundance found in the time-dependent solution (notice that the abundance build-up in time-dependent evolution is synchronized with the iron depletion). Therefore, we are not faced with a contradiction between the time-dependent stationary solution and the equilibrium stratification; they simply result from different physical constraints and are not solutions of the same set of equations (remember that there is no mass conservation in the equilibrium scheme). On the other hand, there are no reasons to believe that solutions are unique in an optically thin medium where solutions do not depend on local abundances. In the present case, the evolution in time of the system has created the hole below  $\log \tau \approx -2.0$  and the atmosphere has converged towards a stationary particle flux before the diffusive flux from deeper layers could fill the hole (larger diffusion time-scale). The time-dependent stationary solution for  $60^\circ$  can be considered more physical than the result of the equilibrium calculation, provided the particles can escape freely from the top of the real atmosphere as they do in our simulation.

#### 4 THE BOUNDARY CONDITION AT THE BOTTOM OF THE ATMOSPHERE

Remember that our boundary conditions are posited such that the iron abundance remains constant with time in the deepest layer. Numerically this choice makes sense, and under the condition that the atmosphere reaches deep enough to ensure diffusion time-scales of the order of the main-sequence lifetime of the star, it would in our opinion also make the best physical choice. Unfortunately, our atmospheres do not reach that deep, so we can expect some dependence of the final stratifications on the optical depth of the lower boundary. In Fig. 2, we plot the final stationary stratifications for atmospheres of 10 000, 11 000 and 12 000 K respectively within  $-4.8 < \log \tau < 2.0$  on the one hand, and within  $-4.8 < \log \tau < 3.0$  on the other hand. Irrespective of the assumed optical depth of the lower boundary, the shapes of the curves remain very much the same; only minor vertical offsets ( $\approx 0.2$  dex) show up.

It might legitimately be objected that in real stellar atmospheres, both effective temperature and gravity change in the course of

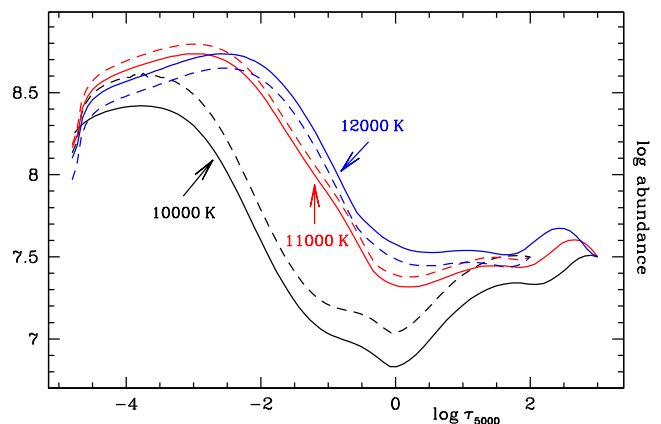


**Figure 2.** Time-dependent diffusion of Fe in three different atmospheres of  $T_{\text{eff}} = 10\,000$ ,  $11\,000$  and  $12\,000$  K, respectively, with  $\log g = 4.0$  and a magnetic field of  $10$  kG strength, inclined by  $60^\circ$  with respect to the surface normal. The curves are labelled with the temperature, the solid lines pertain to atmospheres going down to  $\log \tau = 3.0$  and the dashed lines to those with the lower boundary at  $\log \tau = 2.0$ .

<sup>1</sup> Diffusion velocity may decrease by several orders of magnitude from  $60^\circ$  to  $90^\circ$  in upper layers, see fig. 2 of Alecian (2013b).

<sup>2</sup> The diffusion time-scale is defined as the time needed for particles to diffuse over a pressure scaleheight, and therefore, depends on the diffusion velocity.

the main-sequence evolution of the star, so the lower boundary condition will not stay constant. We therefore have followed the temperature evolution of a  $3 M_{\odot}$  star from 12 290 to 11 900 K over some  $7.5 \times 10^7$  years ( $\log g$  decreases from 4.34 to 4.24). CP stars are often more evolved, since ApBp stars may be found with  $\log g < 3.6$ , but here we present a first attempt at quantifying the effect of evolution. The evolution (not shown) of the Fe stratification is quite similar to the one found for the 12 000 K model in Fig. 2 for the initial  $10^5$ – $10^6$  years; for the remaining time, we find only very minor changes of the order of a few 0.01 dex in the stratification, accompanied by a drop of about 10 per cent in particle flux.

## 5 STRATIFICATIONS AND FIELD STRENGTH

In order to illustrate how the stratifications of the major iron-peak elements behave as a function of magnetic field strength at some given field angle  $\alpha$ , we modelled the simultaneous diffusion of elements 22 to 28 in a  $T_{\text{eff}} = 10\,000$  K atmosphere. The top part of Fig. 3 shows a plot of abundances versus optical depth for  $\alpha = 60^\circ:0$  and 10 000 G (solid lines) and for  $\alpha = 61^\circ:8$  and 1069 G (dash-dotted lines). It may appear somewhat astonishing that abundances near the top of the atmosphere at about  $\log \tau = -4.5$  are *always* larger in the 1 kG case than in the 10 kG case, even though at intermediate optical depths, the opposite is true. The differences in the interval

$-3.0 < \log \tau < 0.0$  tend to reach a maximum of the order of 0.5 dex for Ti, V, Cr, Mn and Co, but are found to be much smaller for Fe and in particular for Ni where they do not exceed 0.15 dex.

It is interesting to have a look at the atmospheric models corresponding to the respective magnetic field strengths. In the bottom part of Fig. 3, we zoom on those layers where the temperature profiles differ. It emerges that the 1 kG field modifies the atmosphere to a larger degree than the 10 kG field. What at first glance could appear counter-intuitive turns out to be due to the effect of a weak field on the diffusion velocities: this occurs in much higher layers than the effect of a strong field, resulting in stronger abundance gradients. Looking at Fe and Cr, which are the most important contributors to line opacity among the iron-peak elements, we note the lower abundances due to diffusion at intermediate optical depths in the 1 kG field, and the higher abundances in the upper atmosphere. The atmosphere has to adapt to these larger gradients by a further increase in temperature in the outer layers, leading in the 1 kG case to a temperature plateau of about 8100 K, centred on  $\log \tau = -2.5$ .

Substantial differences in the shape and slope of unstratified and stratified temperature profiles, respectively, are clearly revealed in Fig. 3 (bottom). The canonical behaviour of atmospheres in the presence of vertically constant overabundances is characterized by the steeper slope of the green curve (short dash-long dashed) with respect to the blue (dashed) curve. The outer layers become cooler as a result of line blanketing as already shown long ago by Chandrasekhar (1935). However, in the presence of very modest underabundances of Fe in intermediate layers, and 1 dex overabundances in higher layers, the picture changes, and the atmosphere reacts with an increase in temperature in the overabundant layers. When the abundance gradient becomes larger, as in the case of the 1 kG field, the temperature increases even further. It would therefore appear that these stratification results cast a shadow of doubt over the validity of abundance analyses – ‘classical’ or by means of Doppler mapping – that rely on unstratified atmospheric models, whether these are based on scaled solar abundances or on individual element abundances.

## 6 INTERACTIONS BETWEEN CHEMICAL ELEMENTS

Stift & Alecian (2012) have shown that considerable interaction can occur between the respective stratifications of the different chemical elements. This can be a consequence of blending, resulting in screening of radiation, and/or as a result of the change in atmospheric structure due to the change in opacity. Let us see what happens for example with Ti: accumulation of this element anywhere in the outer layers of the star will hardly have any effect on the atmosphere or on the other elements. Conversely, even modest overabundances of Fe are known to modify the temperature structure of the atmosphere; in addition, the change in opacity of the countless Fe lines can reduce the amount of radiation available to drive diffusion of Ti. Comparing the final stationary stratification when Ti only is allowed to diffuse, and the stratification of Ti resulting from the simultaneous diffusion of elements Ti, V, Cr, Mn, Fe, Co and Ni, we see quite large differences (Fig. 4). In the particular case of Ti, it would appear that the differences are entirely due to an increase in temperature in the outer layers as suggested by the results of Stift et al. (2013a); possible radiation screening by increased iron line opacity is more than offset by the stronger radiation field inferred from the bottom part of Fig. 3.

Looking at what happens when Fe only is allowed to diffuse, we find results that hardly differ from those obtained with Ti, V, Cr,

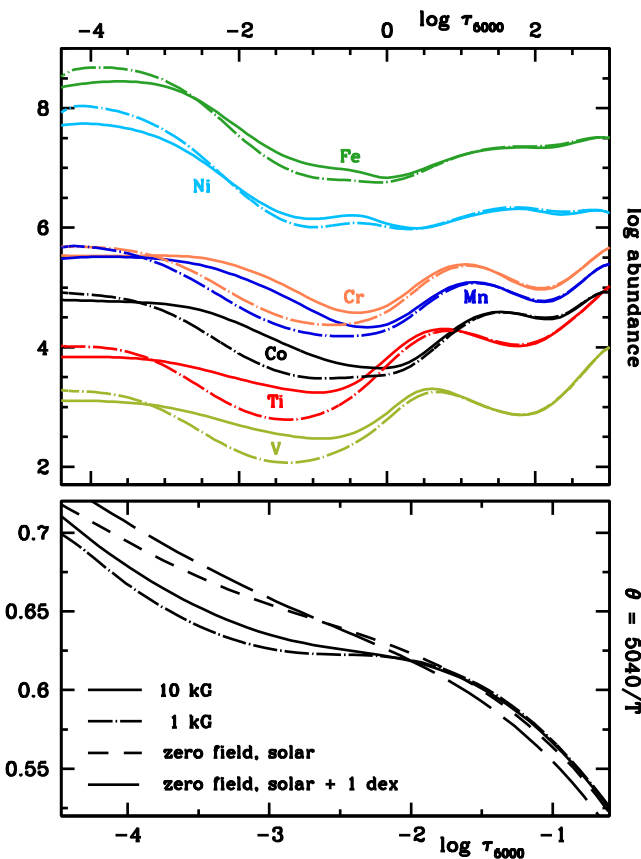


**Figure 3.** Time-dependent diffusion of Ti, V, Cr, Mn, Fe, Co and Ni in a  $T_{\text{eff}} = 10\,000$  K atmosphere. Top: final stationary stratifications as a function of optical depth for field angle  $\alpha = 60^\circ:0$  and 10 000 G (solid line), and for  $\alpha = 61^\circ:8$  and 1069 G (dash-dotted lines). Bottom: inverse temperature  $\theta = 5040/T$  as a function of optical depth for the corresponding stratified atmospheres and for unstratified atmospheres with solar abundances (long dashed) and with solar abundances scaled by +1 dex (short dashed).

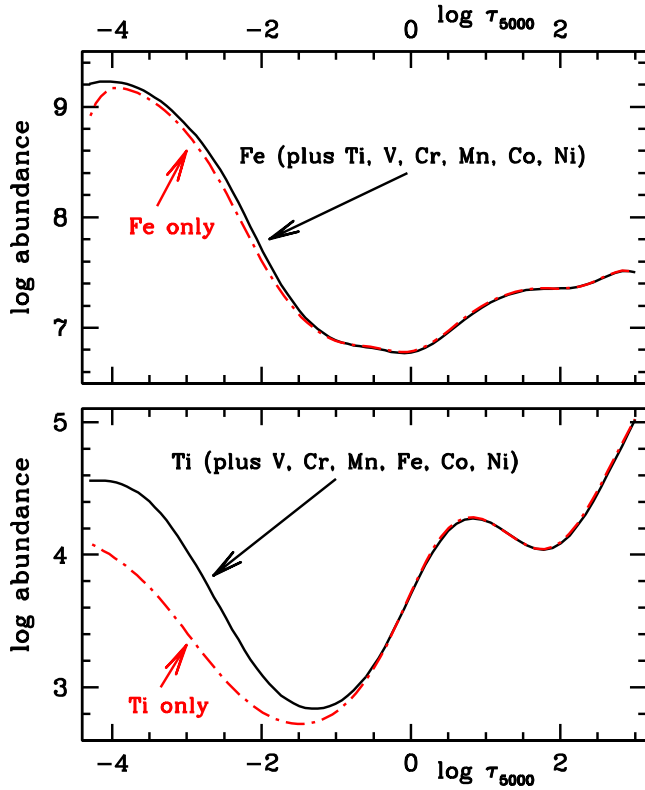


**Figure 4.** Final stationary stratifications of Ti and of Fe, resulting from time-dependent atomic diffusion. Bottom panel: run of the abundance of Ti versus optical depth. The black line pertains to Ti diffusing with V, Cr, Mn, Fe, Co and Ni, and the dash-dotted line to Ti only diffusing. Top panel: same kind of plot for Fe. The black line pertains to Fe diffusing with Ti, V, Cr, Mn, Co and Ni, and the dash-dotted line to Fe only diffusing.

**Table 1.** Magnetic field angle  $\alpha$  with respect to the surface normal and field modulus  $|\mathbf{B}|$  used in the diffusion calculations of elements 22 to 28 as a function of magnetic latitude  $\lambda$ .

$\lambda$ (deg)	$\alpha$ (deg)	$ \mathbf{B} $ (G)	$\lambda$ (deg)	$\alpha$ (deg)	$ \mathbf{B} $ (G)
5.0	80.1	986	25.0	47.0	1208
7.6	75.0	1000	40.0	30.8	1460
10.0	70.6	1018	55.0	19.3	1693
15.0	61.8	1069	90.0	0.0	1950
20.0	54.0	1133			

Mn, Co and Ni all diffusing at the same time. We conclude that the structure of the atmosphere solely depends on the iron stratification, which is not surprising, given the abundance profile of Cr which attains solar values at most.

## 7 STRATIFICATIONS IN A DIPOLE FIELD

In the papers cited previously, very different magnetic field strengths and field angles have been adopted in order to show some instructive examples of how diffusion and abundances develop with time in ApBp star atmospheres. Here instead we want to illustrate the final stationary stratifications to be expected in a simple oblique rotator. For this purpose, we chose a star with a  $T_{\text{eff}} = 10\,000$  K atmosphere and a magnetic field geometry given by a centred dipole with a 1950 G field at the pole – the field angles and strengths are given in Table 1. Again, elements 22 to 28 were allowed to diffuse simultaneously.

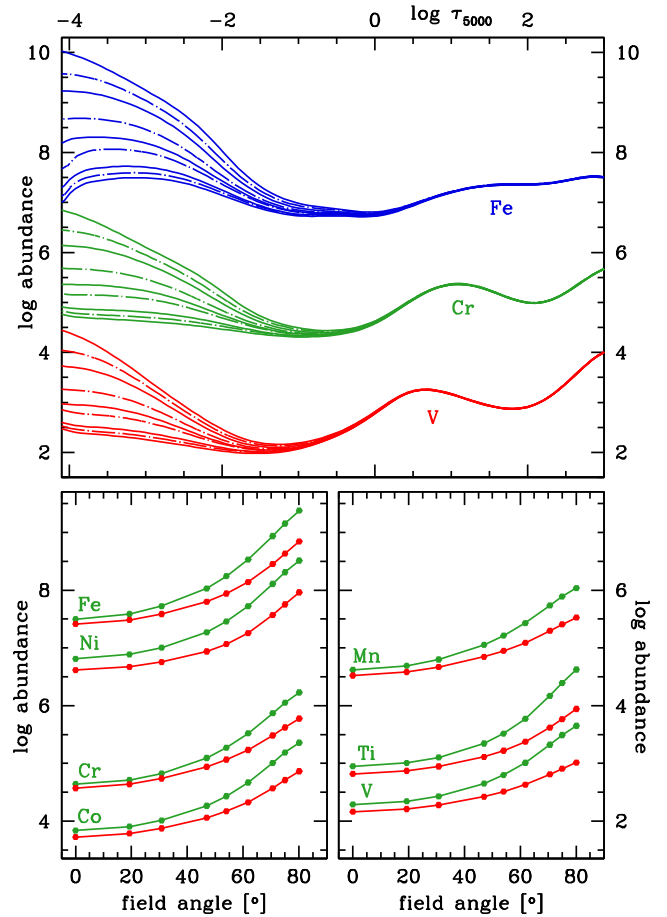


**Figure 5.** Time-dependent diffusion of Ti, V, Cr, Mn, Fe, Co and Ni in a  $T_{\text{eff}} = 10\,000$  K atmosphere. Top: final stationary stratifications of three elements for the field angles  $\alpha$  and corresponding field strengths listed in Table 1. Bottom: final abundances as a function of field angles  $\alpha$  and field strengths at two different optical depths, namely  $\log \tau = -3.156$  (upper curves) and  $\log \tau = -2.575$  (lower curves).

The top part of Fig. 5 shows the final stationary abundance stratifications for V, Cr and Fe as a function of field angle. As one would expect for the modest field strength of about 1 kG at the magnetic equator, the effect of the magnetic field is largely negligible below  $\log \tau = 0$ . In higher layers however we find astonishingly large overabundances of iron at  $80^\circ$  and an increase by still more than 1 dex over the solar value already at  $60^\circ$ . Note that the abundance profile drops towards the highest layers, leading to a kind of stable iron cloud suspended at optical depths that depend on the field angle. The larger the angle, the higher the cloud. At intermediate optical depths, we encounter slight underabundances, something that is also found at the top of the atmosphere in the presence of nearly vertical field lines. Cr displays less important overabundances which hardly attain 1.5 dex, but in contrast to Fe, the underabundances become more pronounced. This trend is enhanced in the case of V which becomes underabundant by up to 2 dex almost throughout the atmosphere, apart from high layers at large field angles.

For a different view of the increase in abundances with field angle  $\alpha$ , we refer to Fig. 5 (bottom part). Both at  $\log \tau = -3.156$  (shown in green) and at  $\log \tau = -2.575$  (shown in red) we find gratifyingly smooth relations which convincingly demonstrate the stability of the numerical scheme employed in CARATSTRATMOTION. In fact, the various calculations started from different initial vertical

abundance distributions: some evolved from solar abundances, others from stratifications for neighbouring angles. Fortunately, the final stationary solutions turn out to be unique, irrespective of the starting abundances. Only a small interval in latitude around the magnetic equator is not covered; it would not appear unreasonable to extrapolate the abundance versus angle relations towards  $90^\circ$ , which can result in quite large overabundances. However, it cannot be excluded that such stratifications will in some cases trigger either hydrodynamical instabilities [for instance due to an inverted  $\mu$  gradient as proposed by Vauclair (2004), or to a temperature inversion] with ensuing mixing, or else that strong radiation screening will lead to the collapse of the stratification (see the unstable scenario proposed by Alecian 1998). Remember on the other hand that the contribution to the observed line profiles is somehow limited since the equatorial ring of unknown abundances is quite narrow. In order not to exaggerate the effects of the temperature profiles and the stratifications, for detailed modelling of line profiles we chose to limit the abundances to the values determined for  $80^\circ$ .

### 7.1 Predicted line profiles

Let us first emphasize that neither do we have the intention nor the possibilities to model a specific star, our grid of stratified models being as yet too sparse for this purpose. In order to illustrate how spectral lines formed in stratified magnetic ApBp star atmospheres may behave, we have chosen to look at moderately strong magnetic fields in a 10 000 K atmosphere, typical for many Sr–Cr–Eu stars (Floquet 1981). We then adopted the moderate projected rotational velocities found in a number of ApBp stars which have been analysed with the help of Doppler imaging (for this technique, see Vogt, Penrod & Hatzes 1987). The choice of spectral lines routinely used in abundance and in Doppler mapping work is quite large; we selected the Fe II lines  $\lambda\lambda 4555.893$  and  $4923.927 \text{ \AA}$ . We finally adopted a centred dipole oblique rotator model (see Stift 1974) with  $70^\circ$  obliquity, a polar field strength of 1950 G, and an inclination of the rotational axis towards the observer of  $i = 57^\circ$  and applied our results obtained for the field angles  $\alpha$  and the field strengths given in Table 1 to this magnetic model. Fig. 6 (top) displays the profile variations of the  $\lambda 4555.893$  line for a projected rotational velocity of  $12.5 \text{ km s}^{-1}$ . In the left-hand panel, we show the profiles that would result from the stratified abundances and modified atmospheres, but without Zeeman splitting; in the right-hand panel, Zeeman splitting is correctly taken into account. The profiles in the magnetic case turn out to be slightly deeper on the average (due to magnetic intensification), with the amplitude of the variations attaining some 5 per cent. It should be noted that the magnetic field does virtually nothing in the way of changing the shapes of the individual phase-dependent profiles, the relative positions of the line cores and the order in phase by which the line depth increases or decreases.

What would the profiles look like if we used equilibrium stratifications instead of the final stationary ones? The answer to this question is given by the profiles labelled ‘equil.’ in the left-hand panel of Fig. 6. At moderate field strengths of 1–2 kG, the contrast in abundance stratifications between vertical and horizontal magnetic fields is very small, resulting in the absence of observable profile variations.

Some interesting behaviour is exhibited by the  $\lambda 4923.927$  line when modelled with a non-axisymmetric tilted eccentric dipole model according to Stift (1975). The assumed decentring parameter of 0.15 (in units of radius) and the obliquity of  $\beta = 57^\circ$  combine to yield a magnetic field modulus ranging between 660 and 2370 G

and *warped* equatorial rings of enhanced abundances – for an idea on what such field geometries can look like, we refer to Stift et al. (2013b). Taking  $v \sin i = 20 \text{ km s}^{-1}$  and an inclination of  $i = 75^\circ$  leads to the profiles shown in Fig. 6 (bottom). The profile variations in the zero field case are found to be so small ( $\approx 1$  per cent) as to be largely swamped by the noise of observed spectra, whereas in the magnetic case a deeper line varies by up to  $\approx 2.5$  per cent. The modification of the line profiles due to the magnetic field is clearly visible: shapes, relative positions and the order in phase all change. This gives one some idea of what the signatures of abundance rings – *warped* rings in the case of the tilted eccentric dipole model of Stift (1975) – following the isoclines of the magnetic field could look like when the appropriate stratifications are taken into account.

## 8 CONCLUSIONS

We have presented new time-dependent diffusion calculations and discussed the dependence of the final stationary stratifications on magnetic field angle and on field strength. It is confirmed that (almost) horizontal fields have a huge impact on the atmospheric structure, that accumulation of Fe in the outer stellar layers can lead to an increase in temperature, to temperature plateaus and even to temperature inversions. Somewhat unexpectedly, these effects tend to be more important for fields of the order of 1 kG than for 10 kG fields. Putting the lower boundary – where the abundances are assumed to remain constant (infinite reservoir) – at different optical depths hardly changes the shape of the stratification profiles, but results in different, moderate offsets. Interactions between the various chemical elements by means of blending or by a changed atmospheric structure are not to be overlooked, underlining the importance of including the most important contributors to line opacity in the diffusion calculations.

As has been known before (Stift et al. 2013a), stationary solutions (with non-zero diffusion flux) can be very different from equilibrium stratifications, going sometimes outright in the opposite sense as in Fig. 1. We have shown how these differences can be understood in terms of boundary conditions and time-scales, but it is difficult to imagine a scenario in which the outgoing diffusion flux at the upper boundary could be forced to go to zero in order to make the time-dependent solution conform with the equilibrium solution. A horizontal field in a highly ionized upper atmosphere could do the job; NLTE effects may also work in a similar sense. However, horizontal fields still constitute an insurmountable difficulty in the time-dependent modelling of diffusion as outlined in the previous sections, and it is not certain that there will not be a pile-up of diffusing elements below the zero-flux region, resulting in huge abundance gradients, temperature inversions and possibly physical instabilities. The importance of NLTE effects (NLTE is not implemented in our codes) for the accelerations of iron-peak elements can roughly be estimated from TLUSTY (Hubeny & Lanz 1995) model atmospheres calculated with the stratifications obtained with our CARATSTRATMOTION code. It turns out (Hubeny, private communication) that the temperature structure changes due to NLTE are very small below  $\log \tau \approx -4$  so that it becomes quite likely that temperature inversions due to atomic diffusion will occur in real ApBp stars.

Concerning the line profile predictions, based on our diffusion calculations, they constitute a starting point for further investigations aimed at establishing whether (warped) rings display unique signatures that differ substantially and unmistakably from those due to unstratified abundance spots. The present results certainly suggest that neglecting the magnetic field in the abundance mapping

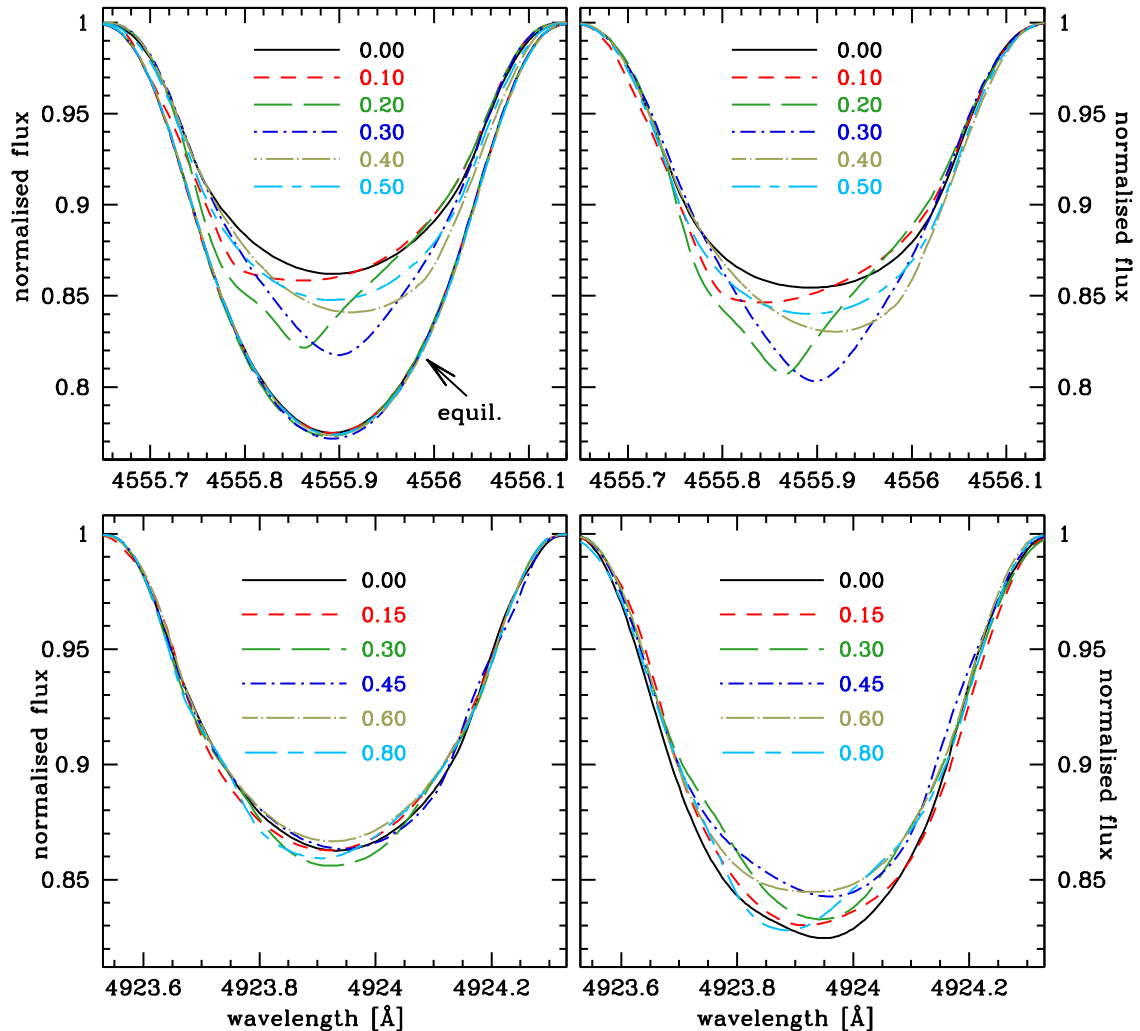


**Figure 6.** Predicted variations with phase of two iron lines, using the magnetic angle-dependent stratified  $T_{\text{eff}} = 10\,000\text{ K}$ ,  $\log g = 4.0$  atmospheres discussed in Section 7. Top: the Fe II line at  $\lambda 4555.893\text{ \AA}$ , modelled with a centred dipole oblique rotator model of inclination  $i = 57^\circ$ , obliquity  $\beta = 70^\circ$  and  $v \sin i = 12.5\text{ km s}^{-1}$ . Left: without Zeeman splitting. For comparison, the profiles calculated from equilibrium stratifications (see Alecian 2015) for the same magnetic geometry are also shown. Right: with Zeeman splitting corresponding to a 2 kG field modulus at the magnetic poles. The lines in black (solid), red (short dashed), green (long dashed), blue (dot–short dashed), khaki (dot–long dashed) and cyan (short dashed–long dashed) correspond to phases 0.00, 0.10, 0.20, 0.30, 0.40, 0.50. Bottom left and right: the Fe II line at  $\lambda 4923.927\text{ \AA}$ . The non-axisymmetric oblique rotator model is characterized by inclination  $i = 75^\circ$ , obliquity  $\beta = 57^\circ$ , decentring parameter 0.15 (in units of radius) and  $v \sin i = 20\text{ km s}^{-1}$ . The symbols are the same as above but the phases are now 0.00, 0.15, 0.30, 0.45, 0.60, 0.80.

of ApBp star, as has been done a number of times in recent years, may not be justified and that the resulting maps could thus prove spurious. In addition, given the strong dependence of stratification profiles on the magnetic field angle, it must be admitted that the validity of the ubiquitous assumption of vertically constant chemical abundances in Doppler mapping can no longer be taken as granted. More diffusion calculations and a large number of inversions with as many different predicted line profiles as possible will be needed to clarify these points.

#### ACKNOWLEDGEMENTS

We want to thank Dr Ivan Hubeny for help in clarifying NLTE issues. GA acknowledges the financial support of the Programme National de Physique Stellaire (PNPS) of CNRS/INSU, France. MJS and GA are grateful for support from the Observatoire de

Paris-Meudon. Thanks go to AdaCore for providing the GNAT GPL Edition of its Ada compiler.

#### REFERENCES

- Alecian G., 1998, *Contrib. Astron. Obs. Skalnaté Pleso*, 27, 290  
Alecian G., 2013a, in Alecian G., Lebreton Y., Richard O., Vauclair G., eds, *EAS Publ. Ser. Vol. 63, New Advances in Stellar Physics: From Microscopic to Macroscopic Processes*. EDP Sciences, Les Ulis, p. 219  
Alecian G., 2013b, in Shibahashi H., Lynas-Gray A. E., eds, *ASP Conf. Ser. Vol. 479, Progress in Physics of the Sun and Stars: A New Era in Helio- and Asteroseismology*. Astron. Soc. Pac., San Francisco, p. 35  
Alecian G., 2015, *MNRAS*, 454, 3143  
Alecian G., Stift M. J., 2006, *A&A*, 454, 571  
Alecian G., Stift M. J., Dorfi E. A., 2011, *MNRAS*, 418, 986  
Babel J., Michaud G., 1991, *A&A*, 248, 155  
Bischof K. M., 2005, *Mem. Soc. Astron. Ital. Suppl.*, 8, 64  
Chandrasekhar S., 1935, *MNRAS*, 96, 21

- Floquet M., 1981, *A&A*, 101, 176  
Hubeny I., Lanz T., 1995, *ApJ*, 439, 875  
Kurucz R. L., 2005, *Mem. Soc. Astron. Ital. Suppl.*, 8, 14  
LeBlanc F., Monin D., Hui-Bon-Hoa A., Hauschildt P. H., 2009, *A&A*, 495, 937  
Michaud G., 1970, *ApJ*, 160, 641  
Proffitt C. R., Brage T., Leckrone D. S., Wahlgren G. M., Brandt J. C., Sansonetti C. J., Reader J., Johansson S. G., 1999, *ApJ*, 512, 942  
Seaton M. J., 1999, *MNRAS*, 307, 1008  
Stift M. J., 1974, *MNRAS*, 169, 471  
Stift M. J., 1975, *MNRAS*, 172, 133  
Stift M. J., Alecian G., 2012, *MNRAS*, 425, 2715  
Stift M. J., Alecian G., Dorfi E. A., 2013a, in Alecian G., Lebreton Y., Richard O., Vauclair G., eds, *EAS Publ. Ser. Vol. 63, New Advances in Stellar Physics: From Microscopic to Macroscopic Processes*. EDP Sciences, Les Ulis, p. 227  
Stift M. J., Hubrig S., Leone F., Mathys G., 2013b, in Shibahashi H., Lynas-Gray A. E., eds, *ASP Conf. Ser. Vol. 479, Progress in Physics of the Sun and Stars: A New Era in Helio- and Asteroseismology*. Astron. Soc. Pac., San Francisco, p. 125  
Turcotte S., Richer J., Michaud G., 1998, *ApJ*, 504, 559  
Vauclair S., 2004, in Zverko J., Ziznovsky J., Adelman S. J., Weiss W. W., eds, *Proc. IAU Symp. 224, The A-Star Puzzle*. Cambridge Univ. Press, Cambridge, p. 161  
Vauclair S., Hardorp J., Peterson D. M., 1979, *ApJ*, 227, 526  
Vogt S. S., Penrod G. D., Hatzes A. P., 1987, *ApJ*, 321, 496

This paper has been typeset from a  $\text{\TeX}/\text{\LaTeX}$  file prepared by the author.